Surface Micromachined Integrable High Efficiency Ridge Gap Waveguide Bandpass Filter for G-Band 6G Applications

Alexander Wilcher
Electrical and Computer Engineering
University of Florida
Gainesville, United States
wilcheralexander@ufl.edu

Alex Phipps
Naval Information Warfare Center (NIWC) Pacific
San Diego, United States
alex.g.phipps.civ@us.navy.mil

Hae-In Kim
Electrical and Computer Engineering
University of Florida
Gainesville, United States
kimhaein@ufl.edu

Jia Chieh
Naval Information Warfare Center (NIWC) Pacific
San Diego, United States
jiachi.s.chieh.civ@us.navy.mil

Yong-Kyu Yoon
Electrical and Computer Engineering
University of Florida
Gainesville, United States
ykyoon@ece.ufl.edu

Ziqi Jia
Electrical and Computer Engineering
University of Florida
Gainesville, United States
jia.ziqi@ufl.edu

David Arnold
Electrical and Computer Engineering
University of Florida
Gainesville, United States
darnold@ufl.edu

2023 IEEE 73rd Electronic Components and Technology Conference (ECTC) | 979-8-3503-3498-2/23/$31.00 ©2023 IEEE | DOI: 10.1109/ECTC51909.2023.00254

***Abstract*— This paper presents a third-order band pass filter (BPF) ridge gap waveguide (RGWG) fabricated utilizing the combination of SU-8 polymer and a photolithography and subsequent metallization process. The RGWG device is designed, simulated, and fabricated to operate in the G-band (110 - 300 GHz) frequency range. With a center frequency of 167 GHz, the fabricated devices have average surface roughness and fabrication tolerances less than 100 nm and 25 µm in all three dimensions, respectively, which are significantly smaller than those of computer numerically controlled (CNC) fabricated devices, e.g. greater than 300nm and 50 µm respectively. The micromachined SU-8 based devices in simulation show 0.87 dB insertion loss at a center frequency of 167 GHz with a 7.5% fractional bandwidth (FBW). Realized the BPF-RGWG device has potential for use in high-frequency applications such as satellite communication and millimeter-wave imaging systems.**

Keywords—Micromachining, High-frequency, Band pass filter, Ridge gap waveguide

I. Introduction

The current technological trend of moving toward millimeter wave technologies is spurred by "an insatiable demand for information" [1]. The development and deployment of fourth-generation (4G) communication systems, followed by fifth-generation (5G) communication systems, best highlight this trend [1]. The strongest evidence of this trend toward millimeter wave frequencies, however, is the roadmap toward future sixth generation (6G) communication technologies. This trend is expected to dramatically change the way society communicates and accesses information, and to realize these future millimeter-wave technologies, much research and technological progress must be done. The need for compact narrowband filters at millimeter wave frequencies currently opens opportunities for exploration and progress in this area [2], [3].

The RGWG design is advantageous at millimeter wave frequencies due to its high power handling capabilities, enclosed nature, low propagation loss, and resilience against electromagnetic interference [3]. Aside from those advantages, the possibility of miniaturization and integration with new and existing components make the RGWG design worth investigating. The RGWG technology presented in this paper consists of several components, the first of which is a metamaterial acting as an artificial perfect magnetic conductor (PMC). The artificial PMC utilized in this design is sometimes referred to as "Fakir's bed of nails" and is in common use due to its ease of design and negligible losses [2]. The use of the bed of nails technology has been demonstrated a number of times in a range of different applications successfully. When the surface created by this artificial PMC is placed in parallel with a surface consisting of a perfect electrical conductor (PEC), an electromagnetic band gap (EBG) is formed, and propagation within a designed band is prevented [4], [5]. To guide and confine a propagating signal between the two regions, a conductive ridge acting as a second PEC is added in the middle of the PMC, effectively splitting it into two halves [2]. The wave will be guided by the ridge and the PEC plate above while being confined due to the presence of the PMCs on either side of the ridge. Within this ridge, grooves are cut to create half-wavelength resonators that are capacitively coupled to create the pass band of the designed narrow filter [6]. Transitions between the RGWG device and transmission structures include microstrip, coplanar waveguide, and step-ridge transitions [5-7]. The use of these individual components in a third order band pass filter design together exhibits low insertion loss and high out-of-band rejection, making it suitable for use in communication and radar systems. Fig. 1 depicts the proposed RGWG device that incorporates these various architectures.

2377-5726/23/$31.00 ©2023 IEEE
DOI 10.1109/ECTC51909.2023.00254

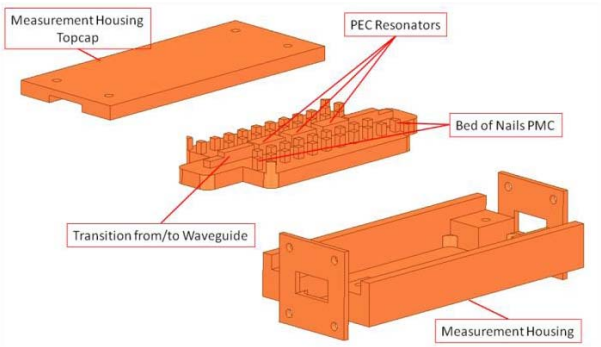

Fig. 1. Topology of the proposed RGWG with band pass filtering functionality.

Manufacturing is one of the current challenges to the widespread use and adoption of RGWG for millimeter wave applications. The most significant challenge is related to the fact that feature sizes and manufacturing tolerances of devices continue to decrease with increasing frequency. This is due to the structures being geometrically dependent on the wavelength of a given frequency [2]. As such, at higher frequencies, certain manufacturing tolerances that are negligible at low frequencies, such as surface roughness, take on new significance, as will be elaborated in a later section. These manufacturing challenges have necessitated the continued use of substrate bound transmission lines at high frequencies, which themselves observe high losses at these high frequencies [8]. Millimeter-wave components that are not substrate bound are commonly fabricated using a CNC milling approach [6][9]. The CNC approach has drawbacks with limited patterning resolution due to drill bit physical dimensions and surface roughnesses in the micrometer range. Additionally, the significant costs and time associated with using a CNC milling approach may hinder the development of RGWG technologies for millimeter wave applications.

II. Surface Roughness Effects

The surface roughness of fabricated devices is of greater importance at millimeter wave frequency than at lower frequencies. There are two common models used to quantify the surface roughness related loss: the Groiss model and the Hurray snowball model [10], [11]. The Groiss model is a semi-empirical model that relates the skin depth (δ_s) and the surface roughness (h) to produce a factor (C_s) to take surface roughness into account.

$$C_s = 1 + \exp\left(-\left(\frac{\delta_s}{2h}\right)^{1.6}\right) \quad (1)$$

This factor is then used to determine the surface admittance of the conductor [10]. As can be seen in equation (1), as skin depth decreases to equal to or less than the surface roughness, the factor increases. Since skin depth decreases with increasing frequency, the surface roughness losses will increase with frequency for a constant surface roughness. The Hurray model describes surface roughness loss as the scattering of the electromagnetic fields due to the creation of magnetic and electric dipole moments by modeling the roughness as conductive spheres. Equation (2), shows the ratio σ_{sc} of the power lost (ΔP_i) due to scattering of the incident power (P_{inc}) where (σ_{sc}) is the scattering cross section, and (a_i) the radius of the conductive sphere.

$$\frac{\Delta P_i}{P_{inc}} = \sigma_{sc} = \frac{15}{8\pi}\left(\frac{\omega^4}{c_2^4}\right)\left(\frac{4\pi a_i^3}{3}\right)^2 \quad (2)$$

From this model, it is also clear that at higher frequencies, the power losses at a fixed surface roughness described by the sphere's radius increase and become a challenge to be addressed. Techniques to reduce the effects of surface roughness have been and are currently being explored. Chemical mechanical polishing (CMP) is one such established and widely adopted method of reducing surface roughness; however, like other methods, it has constraints such as planarization that may make it difficult for use with RGWG type devices. Simulations of the RGWG device have been carried out using Ansys High Frequency Structure Simulator (HFSS) software, utilizing the Groiss model due to its ease of use as compared to the Hurray model. Fig. 2 shows the insertion loss as a function of the surface roughness at the device's center frequency of 167 GHz.

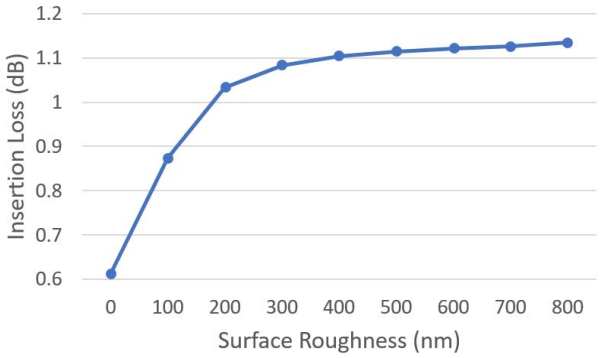

Fig. 2. HFSS simulation results of the insertion loss of a device with different surface roughness values at 167 GHz.

As can be seen from the simulation results at millimeter wave frequencies, surface roughness must be considered to achieve optimal performance and minimize insertion loss.

III. Fabrication

To remedy these manufacturing challenges, an epoxy-based negative photoresist SU-8, which is commonly used in the fabrication of microelectromechanical (MEMS) devices, is utilized to pattern the backbone of the RGWG device with greater precision and lower surface roughnesses. The fabrication process shown in Fig. 3 began with the sputter disposition of 100 nm titanium (Ti) onto a 2 inch silicon (Si) wafer.

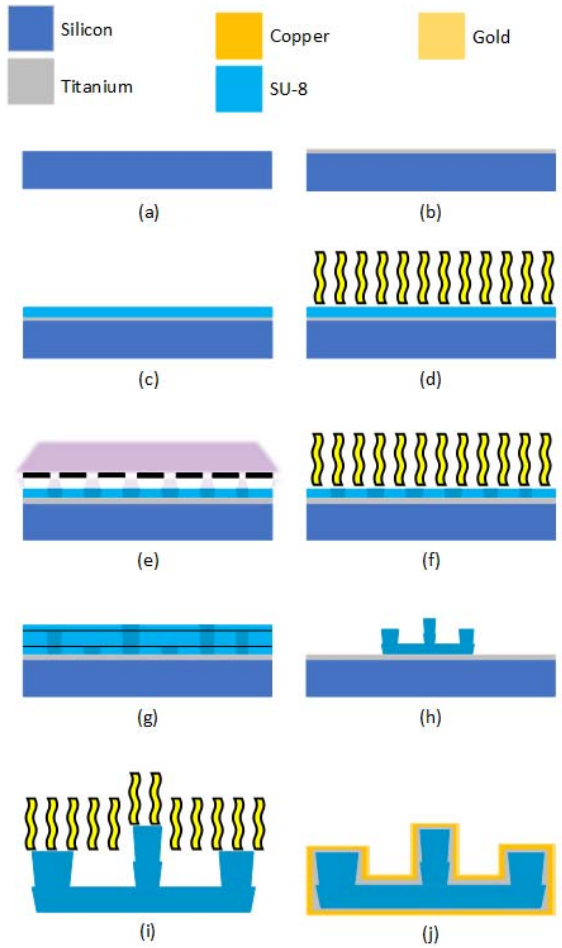

Fig. 3. Fabrication Procedure (a) Si wafer, (b) Ti release layer sputtered, (c) first layer of SU-8 dispensed, (d) soft bake, (e) patterning & exposure, (f) post exposure bake, (g) repeat steps c-f for additional layers, (h) development of the SU-8, (i) release and hardbake/cure of SU-8, and (j) sputtering of Ti, Cu, Au.

The Si wafer acts as the fabrication substrate, and the Ti is used as a released or sacrificial layer further along in the fabrication process. With the substrate prepared, SU-8 2005 is distributed onto the substrate by weight onto the fabrication substrate by pipette. The approximately 20 cm² area of the substrate, desired thickness, density of the SU-8 solution, and amount of solids versus solvent in the SU-8 are used to determine the weight of SU-8 to be poured onto the substrate to realize desired layer thicknesses. This is then followed by a 3 hour soft bake at 95 °C on a hot plate. It is critical that the hot plate be leveled prior to this step, as an unleveled surface leads to variation of the SU-8 thickness across the substrate. Exposure is done with a 395 nm light source using a dosage of around ~1.5x that found in SU-8 2005's data sheet, this is done to achieve a near vertical profile. Spacers must be used during exposure to keep the SU-8, which is still tacky after the soft bake from sticking to the exposure masks; the use of spacers requires accounting for the dispersion of the exposure source to achieve accurate width and length dimensions. A post exposure bake (PEB) of 15 minutes at 85 °C in an oven completes the first device layer. The steps from distributing SU-8 to PEB are repeated for every subsequent layer. Once the last layer is complete, a ~24 hour relaxation period is required to prevent fissures in the SU-8 during development. Development is performed by SU-8 developer using agitation provided by a stir bar rotating at 150 rpm until structures are visibly sharp and no residue is visible. Following that, the sample is rinsed with fresh developer to remove any partially developed SU-8 particulates from the device structures. The developed substrates are then submerged in diluted hydrofluoric acid (HF) until device structures are released from the fabrication substrates. The time for the devices to be released depends on the concentration of HF in the diluted solution. A dilution of HF to deionized water of 1:50 takes 2 days for release. Once released, the devices are then baked at 85 °C for 30 minutes in an oven to prevent deformation and curling during metal deposition. Metal deposition is completed using sputtering, starting with 30 nm thick Ti as an adhesion layer, 1 µm thick copper (Cu) as the conducting layer, and 50 nm thick gold (Au) as a passivation layer on both sides of the device structures. One skin depth of Cu at 167 GHz is approximately 160 µm and 5 skin depths are approximately 800 µm. The minimum of five skin depths is used to limit power loss and excessive material usage, hence the 1 µm of Cu. Once completed, the device structures are ready for characterization. In Fig. 4, a scanning electron microscope (SEM) image of a completed device is shown.

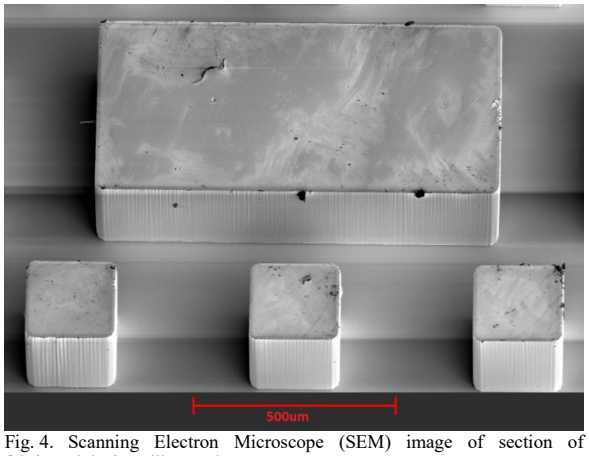

Fig. 4. Scanning Electron Microscope (SEM) image of section of fabricated device pillars and PEC resonator.

IV. Measurments & Results

The dimensions and the average surface roughness are measured using a Bruker Contour GT-I optical profilometer using phase-shifting interferometry using a 135 nm source, this methods allows for the measurement of surface roughnesses below 30 nm. A comparison of devices fabricated using the CNC method and the SU-8 method using the Bruker profilometer and an optical microscope is shown in Fig 5. From these measurements, the average surface roughnesses in all three dimensions are measured below 100 nm, and the dimensional tolerances are below 25 µm. Considering CNC milling machines are limited by the dimensions of the drill bit used and surface roughnesses in the micrometer range, this represents a significant improvement.

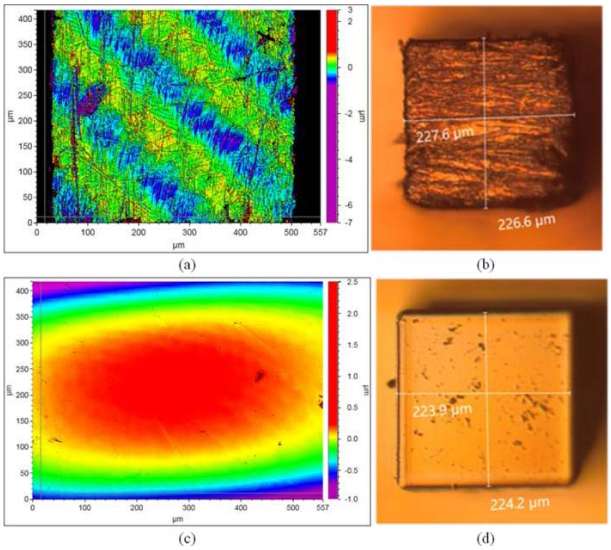

Fig. 5. (a) Colormap of top surface of pillar fabricated using CNC process with data obtained from optical profilemeter (b) Optical microscope image of bed of nail pillar fabricated using CNC process, (c) colormap of top surface of pillar fabricated using SU-8 process with data obtained from optical profilemeter, and (d) Optical microscope image of bed of nail pillar fabricated using SU-8 process

The scattering parameters of the device are measured using the previously mentioned measurement housing connected to a VDI WR5.1 VNA extender, as shown in Fig. 6. This is then connected to an Anritsu 37347C vector network analyzer.

Fig. 6. Measurement setup

These measurements are ongoing, and the measurement results will be presented at the conference. The s-parameter measurements that have been obtained showed a band pass response at the simulated center frequency with a FBW similar to that simulated. However, the devices showed losses much greater than those simulated. This is suspected to be due to a mismatch in the size of the device's first layer and the housing recess to hold the device, which is leading to greater reflection. More work is needed on fabricating corrected devices by reducing the overall footprint while keeping the same performance and thereby correcting the cause of excessive reflections and insertion losses. The simulated results show a 0.87 dB IL, a center frequency of 167 GHz, and a 7.5% FBW.

V. Discussion & Conclusions

We demonstrate a third order BPF RGWG in the G-band range for millimeter wave applications, which are micromachined using SU-8 photolithography followed by metallization. The structure is fabricated using a three layer SU-8 process. This process is successful at improving the fabrication tolerances and surface roughness as characterized by a profilometer. The feasibility of both the RGWG technology and fabrication techniques is presented here for millimeter-wave applications. The fabrication of the third order BPF RGWG using the fabrication techniques demonstrated here may present a viable option for other millimeter-wave applications of a similar nature. Scattering parameters will subsequently be measured and compared to the simulated results and the results from a device fabricated using a CNC approach.

Acknowledgment

This work has been supported by the Multi-functional Integrated System Technology (MIST) Center and
Naval Information Warfare Center (NIWC) Pacific.
The authors are thankful for their support and even more so for their mentorship.

References

[1] dcadmin, "2015 International Technology Roadmap for Semiconductors (ITRS)," *Semiconductor Industry Association*, 2015. https://www.semiconductors.org/resources/2015-international-technology-roadmap-for-semiconductors-itrs/

[2] E. Rajo-Iglesias, M. Ferrando-Rocher and A. U. Zaman, "Gap Waveguide Technology for Millimeter-Wave Antenna Systems," in *IEEE Communications Magazine*, vol. 56, no. 7, pp. 14-20, July 2018, doi: 10.1109/MCOM.2018.1700998.

[3] M. S. Sorkherizi, A. Khaleghi and P. -S. Kildal, "Direct-Coupled Cavity Filter in Ridge Gap Waveguide," in *IEEE Transactions on Components, Packaging and Manufacturing Technology*, vol. 4, no. 3, pp. 490-495, March 2014, doi: 10.1109/TCPMT.2013.2284559.

[4] P. -S. Kildal, E. Alfonso, A. Valero-Nogueira and E. Rajo-Iglesias, "Local Metamaterial-Based Waveguides in Gaps Between Parallel Metal Plates," in *IEEE Antennas and Wireless Propagation Letters*, vol. 8, pp. 84-87, 2009, doi: 10.1109/LAWP.2008.2011147.

[5] Z. Liu, H. Xia, H. Liu and L. Li, "Slow Wave Gap Waveguide With Bandpass Filtering Functionality," in *IEEE Microwave and Wireless Components Letters*, vol. 32, no. 8, pp. 953-956, Aug. 2022, doi: 10.1109/LMWC.2022.3162610.

[6] J.C.S. Chieh, H.D. Ngo, and A. Phipps, "A G-band ridge gap waveguide bandpass filter using CNC machining," IEP Letter

[7] S. Rahiminejad *et al*., "100 GHz SOI gap waveguides," *2013 Transducers & Eurosensors XXVII: The 17th International Conference on Solid-State Sensors, Actuators and Microsystems (TRANSDUCERS & EUROSENSORS XXVII)*, Barcelona, Spain, 2013, pp. 510-513, doi: 10.1109/Transducers.2013.6626815.

[8] P.-S. Kildal, Ed., "WAVEGUIDES AND TRANSMISSION LINES IN GAPS BETWEEN PARALLEL CONDUCTING SURFACES," Jun. 01, 2021 Accessed: Jun. 15, 2022. [Online]. Available: https://patents.google.com/patent/US20110181373A1/en

[9] J. -Q. Ding, S. -C. Shi, K. Zhou, D. Liu and W. Wu, "Analysis of 220-GHz Low-Loss Quasi-Elliptic Waveguide Bandpass Filter," in *IEEE Microwave and Wireless Components Letters*, vol. 27, no. 7, pp. 648-650, July 2017, doi: 10.1109/LMWC.2017.2711544.

[10] S. Groiss, I. Bardi, O. Biro, K. Preis and K. R. Richter, "Parameters of lossy cavity resonators calculated by the finite element method," in *IEEE Transactions on Magnetics*, vol. 32, no. 3, pp. 894-897, May 1996, doi: 10.1109/20.497385.

[11] P. G. Huray *et al*., "Fundamentals of a 3-D "snowball" model for surface roughness power losses," *2007 IEEE Workshop on Signal Propagation on Interconnects*, Genova, 2007, pp. 121-124, doi: 10.1109/SPI.2007.4512227